ChemComm

COMMUNICATION

View Article Online
View Journal | View Issue

Cite this: *Chem. Commun.*, 2017, 53, 12116

Received 4th May 2017,
Accepted 15th August 2017

DOI: 10.1039/c7cc03462h

rsc.li/chemcomm

Measurement of ^{14}N quadrupole couplings in biomolecular solids using indirect-detection ^{14}N solid-state NMR with DNP†

J. A. Jarvis,‡[a] I. Haies, §[b] M. Lelli, ¶[c] A. J. Rossini, ‖[c] I. Kuprov,[b] M. Carravetta[b] and P. T. F. Williamson *[a]

The quadrupolar interaction experienced by the spin-1 ^{14}N nucleus is known to be extremely sensitive to local structure and dynamics. Furthermore, the ^{14}N isotope is 99.6% naturally abundant, making it an attractive target for characterisation of nitrogen-rich biological molecules by solid-state NMR. In this study, dynamic nuclear polarization (DNP) is used in conjunction with indirect ^{14}N detected solid-state NMR experiments to simultaneously characterise the quadrupolar interaction at multiple ^{14}N sites in the backbone of the microcrystalline protein, GB3. Considerable variation in the quadrupolar interaction (>700 kHz) is observed throughout the protein backbone. The distribution in quadrupolar interactions observed reports on the variation in local backbone conformation and subtle differences in hydrogen-bonding; demonstrating a new route to the structural and dynamic analysis of biomolecules.

Nitrogen is an important element in chemistry due to its prevalence in biological and naturally occurring materials. However, solid-state NMR (ssNMR) studies of the 99.6% naturally abundant ^{14}N isotope are challenging principally due to the integer spin number (I = 1) and moderate electric quadrupole moment of the ^{14}N nucleus. This results in ^{14}N spectra that are anisotropically broadened by the first order quadrupolar interaction to several MHz, rendering the ^{14}N isotope difficult to manipulate and detect with ssNMR. Accordingly, ssNMR studies typically favour the spin-1/2 nucleus ^{15}N. The quadrupolar interaction is, however, extremely sensitive to the local structure and dynamics experienced at the ^{14}N site, and its characterisation could provide a wealth of information not readily available from the spectra of the more commonly studied ^{15}N isotope.[1–3] One area where ^{14}N NMR may offer significant benefits is in the field of protein ssNMR. The quadrupolar interaction experienced by each of the amide nitrogens in the peptide backbone is potentially a sensitive reporter to the backbone conformation, secondary structure and dynamics. Indeed evidence from small model peptides indicates that differences in the nature of hydrogen bonding between α-helical and β-sheets conformers can result in significant differences in the magnitude of the ^{14}N electric field gradient (EFG) at the amide nitrogen, regardless of the type of residue.[1,4] Furthermore, the analysis of natural abundance ^{14}N in proteins opens new avenues for the study of complex medical and environmental samples that cannot be labelled for NMR studies.[3]

A number of strategies have been developed in order to characterise the ^{14}N quadrupolar interaction (QI) in a variety of organic and biological materials. These include direct detection of static wideline ^{14}N ssNMR spectra with broadband excitation methods.[5–9] Alternatively, the ^{14}N overtone transition may also be directly detected since this can potentially provide improved resolution[10–14] and sensitivity[15,16] since the overtone transition is unaffected by the first order quadrupolar interaction. Several methods have also been proposed for indirectly detecting ^{14}N that employ a spin-1/2 "spy" nucleus such as ^{13}C or ^{1}H to indirectly detect the fundamental ^{14}N transition in a 2D experiment.[2,17–24] The indirect detection strategy is perhaps the most promising for application to complex molecules with multiple ^{14}N sites since it benefits from the resolution and sensitivity of the "spy" nucleus, and does not suffer the low excitation bandwidth of overtone methods. We have recently reported a technique for such indirect detection that exploits moderate rf fields close to the ^{14}N Larmor frequency, as opposed to a period of free evolution as proposed by a number of other groups,[2,17–22] to generate coherence between the ^{14}N and spy nuclei.[24]

[a] *Biological Sciences, University of Southampton, Southampton, SO17 1BJ, UK. E-mail: p.t.williamson@soton.ac.uk*
[b] *Chemistry Department, University of Southampton, Southampton, SO17 1BJ, UK*
[c] *Centre de RMN à Tres Hauts Champs, Institut de Sciences Analytiques, Université de Lyon (CNRS/ENS Lyon/UCB Lyon1), 69100 Villeurbanne, France*

† Electronic supplementary information (ESI) available: Detailed protocols for sample preparation and NMR data acquisition. Discussion on distribution of 14N shifts and resolution of sites in cryogenic DNP spectra. See DOI: 10.1039/c7cc03462h

‡ Current address: Department of Life Sciences, Imperial College London, London, UK.
§ Current address: Department of Chemistry, Mosul University, Mosul, Iraq.
¶ Current address: Center for Magnetic Resonance, University of Florence, Via L. Sacconi 6, 50019 Sesto Fiorentino, Italy.
‖ Current address: Department of Chemistry, Iowa State University, 0205 Hach Hall, 2438 Pammel Drive, Ames, US.

In this communication we demonstrate the feasibility of recording $^{13}C/^{14}N$ correlation spectra in a full-length protein using such an indirect detection scheme, allowing the determination of the distribution of ^{14}N quadrupolar couplings throughout the protein backbone of third IgG-binding domain of Protein G (GB3).

Dynamic nuclear polarization (DNP) offers significant improvements in sensitivity over conventional MAS-NMR,[25,26] aiding many biomolecular NMR studies.[27] Here we have applied high field MAS-DNP at a field of 18.8 T with sample temperatures of *ca.* 110 K in conjunction with 2D $^{13}C/^{14}N$ correlation spectra to enhance sensitivity and obtain spectra of a microcrystalline preparation of ^{13}C-labelled GB3. Full experimental details are provided in the ESI.† For DNP measurements, two microcrystalline samples of GB3 were incubated with either 2 or 12.5 mM of the biradical AMUPol[28] in glycerol-d_8/D_2O (70 : 30 v/v). In the $^{1}H/^{13}C$ cross polarization (CP) spectra of these two samples, shown in Fig. 1A and B, DNP enhancements ($\varepsilon_{on/off}$) of 3 and 18 were observed, respectively with relatively uniform enhancements throughout the spectrum, something mirrored in the corresponding proton-spin diffusion spectrum (ESI,† Fig. S2). Compared to spectra acquired at 273 K, a significant decrease in resolution is observed due to inhomogeneous broadening that arises upon freezing, although the resolution is favourable when compared to spectra of the homologous protein GB1 at 100 K[29] (Experimental details and a discussion on the resolution observed can be found in the ESI†).

The ^{14}N filtered ^{13}C spectra are shown in Fig. 1C and D. In contrast to the $^{1}H/^{13}C$ CP-MAS spectra, the ^{14}N filtered ^{13}C signal shows only the ^{13}C resonances of nuclei bound to a ^{14}N spin. Furthermore, we notice that the ^{14}N filtered ^{13}C spectrum is more intense at lower radical concentration, with a 10-fold improvement in signal intensity of the 2 mM AMUPol sample over the 12.5 mM AMUPol sample, when expressed as a fraction of the ^{13}C spin echo signal under identical conditions. Typically, attenuation of the signal in the sample at high biradical concentrations is attributed to the enhanced T_2' relaxation arising from the presence of the biradicals in the sample. Here however ^{14}N filtered intensities are compared to a ^{13}C spin-echo signal whose refocusing periods match the duration of the ^{14}N pulses, thereby compensating for any loss in signal due to increased ^{13}C T_2' relaxation. This leads us to speculate that the attenuated signal observed at higher biradical concentrations arises through the enhanced relaxation of the multiple spin ^{14}N–^{13}C coherences during the rf driven recoupling This demonstrates the need to understand how DNP reagents influence the efficiency of different pulse sequences.[30,31] To assess the feasibility of conducting these experiments in the absence of DNP, measurement have made of both microcrystalline and lyophilised material where a greater amount of protein can be packed into the rotor. In the latter case a 1D ^{14}N filter ^{13}C spectrum could be acquired in ~1 week, making 2D acquisition unrealistic.

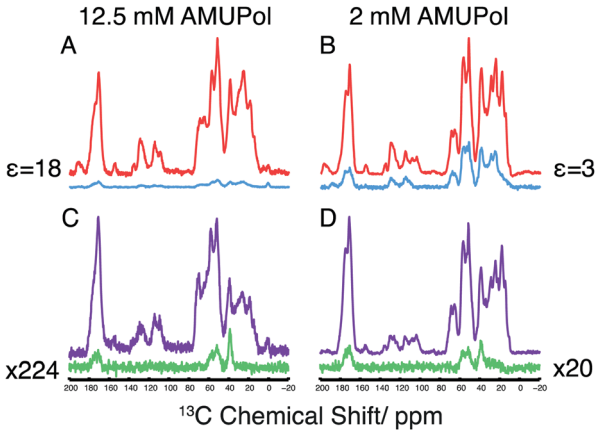

Fig. 1 DNP enhancements and ^{14}N transfer efficiencies recorded from ~30 mg of GB3 in AMUPol. All spectra recorded at 18.8 T, 100 K with 13.5 kHz MAS. CP-MAS ^{13}C NMR spectra in (A) and (B) were recorded on samples containing 12.5 mM AMUPol and 2 mM AMUPol, respectively. Spectra in red and blue show the intensity of the ^{13}C CP-MAS with and without microwave radiation irradiation respectively. The DNP signal enhancements (ε) are indicated. Spin-echo (purple) and ^{14}N filtered spin-echo experiments (green) recorded with DNP on the same samples containing 12.5 mM (C) and 2 mM (D) AMUPol. ^{14}N filtered echo spectra scaling given with respect to corresponding spin-echo, with identical refocusing periods of 1.7 ms corresponding to the ^{14}N pulse length used in both experiments. The intensity of the spectra in each panel were normalised to reflect an equivalent number of acquisitions, and where necessary, scaled by the factor shown in the figure to aid visualisation.

The $^{14}N/^{13}C$ 2D correlation spectra of GB3 together with the corresponding $^{15}N/^{13}C$ correlation spectra processed to mimic the inhomogeneous broadening apparent in the samples measured with DNP are shown in Fig. 2. The most intense feature in the $^{14}N/^{13}C$ correlation spectra, with ^{14}N shifts between 280 ppm and 320 ppm, is assigned to the primary amines in the lysine sidechain on the basis of the ^{14}N and ^{13}C chemical shifts. In the region corresponding to the Cα and CO chemical shift (50–55 ppm and 170–175 ppm ^{13}C shift, respectively) a broad distribution of ^{14}N resonances are observed between 310 ppm and 420 ppm. The ^{14}N shifts cover a range of 110 ppm, a dispersion almost four times greater than observed in the amide region of the corresponding $^{15}N/^{13}C$ spectra. Notable in their absence, are resonances with ^{13}C chemical shifts of 44–47 ppm arising from the glycine residues in GB3. $^{15}N/^{13}C$ 2D correlation spectra (data not shown) acquired under similar DNP conditions, show little perturbation in the Cα shifts of glycine residues, whilst studies of model peptides have indicated that the 14N QI is similar to that of other amino acids. We suggest that the absence of these resonances is due to the short T_2 of these residues arising from incomplete decoupling of the protons within the CH_2 groups of the glycine residues with the proton decoupling fields available.

The increase in ^{14}N shift dispersion in the $^{14}N/^{13}C$ spectrum of the protein, compared to the ^{15}N spectra, is due to the contribution of the field dependent second order isotropic quadrupolar shift (SOIQS) to the ^{14}N shift, in addition to the usual nitrogen isotropic chemical shift. The ^{14}N SOIQS may be given by:[32]

$$^{14}N\delta_Q^{iso} = \frac{3}{40}\left(\frac{\chi_Q}{\nu_0}\right)^2 \times 10^6 \quad (1)$$

where ν_0 is the Larmor frequency and χ_Q is the quadrupolar product:

$$\chi_Q = C_Q\sqrt{1+\frac{\eta^2}{3}} \quad (2)$$

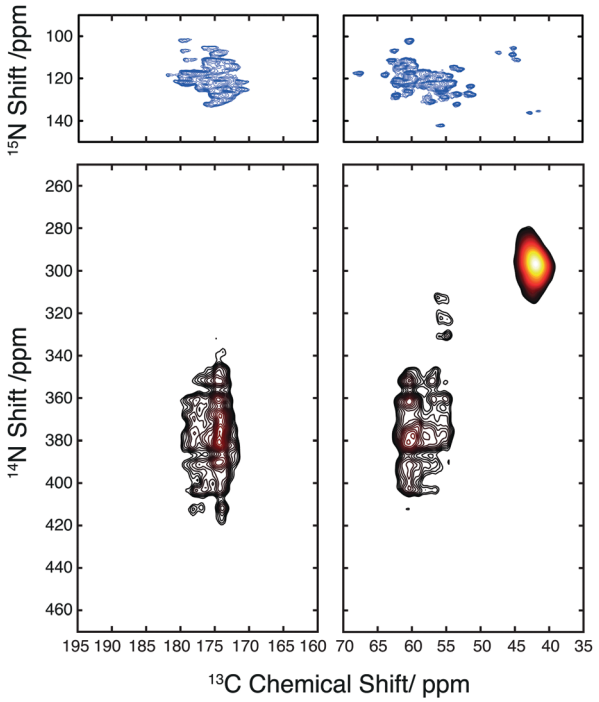

Fig. 2 Carbon/nitrogen correlation spectra of GB3. The top panels show the carbonyl and aliphatic regions of ^{13}C/^{15}N correlation spectra of U-^{13}C,^{15}N-GB3 recorded at 14.1 T, 293 K under 12.5 kHz MAS. Lower panels show corresponding regions of the ^{13}C/^{14}N correlation spectrum of U-^{13}C GB3 containing 2 mM AMUPol recorded at 18.8 T, 100 K under 13.5 kHz MAS.

where C_Q is the quadrupolar coupling constant (typically between 0 and 5 MHz for ^{14}N) and η the asymmetry parameter. While it has not been possible to assign any resonances in the ^{13}C/^{14}N spectrum of GB3 to specific amino acid residues, primarily due to the inhomogeneous broadening observed at 100 K, it is possible to characterise the distribution of quadrupolar couplings present. Subtracting from the centre of the amide region of the ^{14}N spectrum of GB3, 365 ppm, the centre of the amide region of the ^{15}N spectrum, 117.5 ppm, one can determine an "average" amide SOIQS in GB3 of 247.5 ppm at 18.8 T. From eqn (1) and (2), one can determine this to be consistent with C_Q values of 2.88–3.32 MHz, without any knowledge of the asymmetry parameter, η, of the EFG. Similarly, from the 110 ppm (310–420 ppm) distribution of ^{14}N shifts measured at this field, using eqn (1) we can conclude that the ^{14}N C_Q magnitudes present in GB3 span 1.12 MHz, from 2.54 MHz to 3.66 MHz assuming that the asymmetry parameter is undefined. Studies of model peptides typically reveal asymmetry parameters ranging from 0.3 to 0.4[4] for amide bonds in the protein backbone reducing the span of possible to values of C_Q to 724 kHz.

The observed dispersion of C_Q is dependent on both the local dynamics and electronic environment at each of the amide sites in the protein backbone, the latter reflecting the conformation and H-bond status of each site. The magnitude of C_Q measured agrees well with *ab initio* calculations[4] and studies of model compounds including *N*-acetyl-valine,[1] triglycine,[33] and alanyl–glycyl–glycine[17] suggesting the protein backbone is immobile with little overall dynamic averaging of the quadrupolar interaction; as expected for this well-structured protein in a glass-frozen matrix at 100 K.

The dispersion in C_Q is however larger than previous studies of short model peptides, where changes from an α-helical to a β-strand conformation result in a variation of the ^{14}N C_Q of ~200 kHz.[4] The absence of any overall dynamic scaling of C_Q suggests that the larger distribution in C_Q reflects either smaller localised mobility leading to dynamic averaging of C_Q or the greater structural diversity present in the backbone of GB3 compared to earlier studies of model compounds.

To assess whether the dispersion of ^{14}N shifts reflects the distribution of backbone conformations present in GB3 captured here upon sample freezing at 100 K, we have modelled the ^{14}N/^{13}C correlation spectrum based on the SOIQS predicted from the backbone conformations in the crystal structure[34] and the backbone ^{15}N/^{13}C assignment. Qualitatively these modelled spectra mirror the experimental data (see ESI,† Fig. S3), with the intensity in regions where the SOIQS would correlate well with α-helical and β-strands structures. This highlights the potential for such studies to provide an oversight of the secondary structures in proteins.

In conclusion, we demonstrate that combining DNP at cryogenic temperatures with ^{14}N indirect detection it is possible to characterise the quadrupolar interactions at ^{14}N sites within a microcrystalline preparation of GB3. Despite the enhanced linewidths observed under DNP conditions which prohibit the identification of site specific resonances, we have demonstrated the feasibility of characterising the distribution of the quadrupolar interactions through the analysis of the unresolved envelope of ^{14}N resonances in the indirect dimension. The distribution observed reveals that the ^{14}N sites within the protein backbone exhibit a broad range of ^{14}N EFGs that indicate that, in the case of GB3 at these temperatures, the observed shifts reflect the secondary structures adopted by each amino acid. The exquisite sensitivity demonstrated by the EFG to the backbone conformation and the possibility to characterise these sites, offers a novel route to the structural characterisation of biomolecules.

We envision that the utility of this method will be further enhanced through the use of additional dimensions that would alleviate some of the spectra crowding arising from the DNP conditions used. Furthermore, utilization of alternative spy nuclei such as protons would further boost sensitivity whilst facilitating the NMR analysis of biomolecules and other natural products that have previously proved intractable due to difficulties associated with labelling.

This work has been supported by the EPSRC (EP/M023664/1). MC thanks the University Research Fellowship scheme from the Royal Society for support. IH thanks The Higher Committee for Education Development in Iraq for support. The authors acknowledge the use of the IRIDIS HPC Facility at the University of Southampton. Development of Spinach is supported by EPSRC (EP/H003789/1). Financial support by the Access to Research Infrastructures activity in the 7th Framework Programme of the EC (Project number: 261863, Bio-NMR) for conducting the research is gratefully acknowledged. We would like to thank Prof. Emsley and

Dr Lesage for their useful discussion and access to the 800 MHz DNP spectrometer at the ISA, Lyon.

Conflicts of interest

There are no conflicts to declare.

References

1 R. E. Stark, R. A. Haberkorn and R. G. Griffin, *J. Chem. Phys.*, 1978, **68**, 1996.
2 S. Antonijevic and N. Halpern-Manners, *Solid State Nucl. Magn. Reson.*, 2008, **33**, 82–87.
3 G. N. Reddy, M. Malon, A. Marsh, Y. Nishiyama and S. P. Brown, *Anal. Chem.*, 2016, **88**, 11412–11419.
4 J. Fukazawa, S. Kato, T. Ozaki, A. Shoji and K. Takegoshi, *J. Am. Chem. Soc.*, 2010, **132**, 4290–4294.
5 K. J. Harris, S. L. Veinberg, C. R. Mireault, A. Lupulescu, L. Frydman and R. W. Schurko, *Chemistry*, 2013, **19**, 16469–16475.
6 L. A. O'Dell and R. W. Schurko, *J. Am. Chem. Soc.*, 2009, **131**, 6658–6659.
7 L. A. O'Dell and R. W. Schurko, *Phys. Chem. Chem. Phys.*, 2009, **11**, 7069–7077.
8 L. A. O'Dell, R. W. Schurko, K. J. Harris, J. Autschbach and C. I. Ratcliffe, *J. Am. Chem. Soc.*, 2011, **133**, 527–546.
9 S. L. Veinberg, Z. W. Friedl, K. J. Harris, L. A. O'Dell and R. W. Schurko, *CrystEngComm*, 2015, **17**, 5225–5236.
10 L. A. O'Dell and A. Brinkmann, *J. Chem. Phys.*, 2013, **138**, 064201.
11 L. A. O'Dell, R. He and J. Pandohee, *CrystEngComm*, 2013, **15**, 8657.
12 L. A. O'Dell and C. I. Ratcliffe, *Chem. Phys. Lett.*, 2011, **514**, 168–173.
13 Y. Nishiyama, M. Malon, Z. Gan, Y. Endo and T. Nemoto, *J. Magn. Reson.*, 2013, **230**, 160–164.
14 I. M. Haies, J. A. Jarvis, L. J. Brown, I. Kuprov, P. T. F. Williamson and M. Carravetta, *Phys. Chem. Chem. Phys.*, 2015, **17**, 23748–23753.
15 A. J. Rossini, L. Emsley and L. A. O'Dell, *Phys. Chem. Chem. Phys.*, 2014, **16**, 12890–12899.
16 I. M. Haies, J. A. Jarvis, H. Bentley, I. Heinmaa, I. Kuprov, P. T. F. Williamson and M. Carravetta, *Phys. Chem. Chem. Phys.*, 2015, **17**, 6577–6587.
17 Z. H. Gan, *J. Am. Chem. Soc.*, 2006, **128**, 6040–6041.
18 Z. H. Gan, *J. Magn. Reson.*, 2007, **184**, 39–43.
19 S. Cavadini, A. Abraham and G. Bodenhausen, *J. Magn. Reson.*, 2008, **190**, 160–164.
20 S. Cavadini, S. Antonijevic, A. Lupulescu and G. Bodenhausen, *ChemPhysChem*, 2007, **8**, 1363–1374.
21 S. Cavadini, S. Antonijevic, A. Lupulescu and G. Bodenhausen, *J. Magn. Reson.*, 2006, **182**, 168–172.
22 S. Cavadini, V. Vitzthum, S. Ulzega, A. Abraham and G. Bodenhausen, *J. Magn. Reson.*, 2010, **202**, 57–63.
23 Y. Nishiyama, Y. Endo, T. Nemoto, H. Utsumi, K. Yamauchi, K. Hioka and T. Asakura, *J. Magn. Reson.*, 2011, **208**, 44–48.
24 J. A. Jarvis, I. M. Haies, P. T. F. Williamson and M. Carravetta, *Phys. Chem. Chem. Phys.*, 2013, **15**, 7613–7620.
25 Q. Z. Ni, E. Daviso, T. V. Can, E. Markhasin, S. K. Jawla, T. M. Swager, R. J. Temkin, J. Herzfeld and R. G. Griffin, *Acc. Chem. Res.*, 2013, **46**, 1933–1941.
26 T. Maly, G. T. Debelouchina, V. S. Bajaj, K. N. Hu, C. G. Joo, M. L. Mak-Jurkauskas, J. R. Sirigiri, P. C. van der Wel, J. Herzfeld, R. J. Temkin and R. G. Griffin, *J. Chem. Phys.*, 2008, **128**, 052211.
27 Y. Su, L. Andreas and R. G. Griffin, *Annu. Rev. Biochem.*, 2015, **84**, 465–497.
28 C. Sauvee, M. Rosay, G. Casano, F. Aussenac, R. T. Weber, O. Ouari and P. Tordo, *Angew. Chem.*, 2013, **52**, 10858–10861.
29 J. R. Lewandowski, M. E. Halse, M. Blackledge and L. Emsley, *Science*, 2015, **348**, 578–581.
30 D. Lee, S. Hediger and G. De Paepe, *Solid State Nucl. Magn. Reson.*, 2015, **66-67**, 6–20.
31 A. J. Rossini, A. Zagdoun, M. Lelli, D. Gajan, F. Rascon, M. Rosay, W. E. Maas, C. Coperet, A. Lesage and L. Emsley, *Chem. Sci.*, 2012, **3**, 108–115.
32 A. Samoson, *Chem. Phys. Lett.*, 1985, **119**, 29–32.
33 M. Strohmeier, D. W. Alderman and D. M. Grant, *J. Magn. Reson.*, 2002, **155**, 263–277.
34 T. S. Ulmer, B. E. Ramirez, F. Delaglio and A. Bax, *J. Am. Chem. Soc.*, 2003, **125**, 9179–9191.